Hadro-chemistry effects on leptons from charm-hadron decays in heavy-ion collisions

Kai Lu and Min He*

Department of Applied Physics, Nanjing University of Science and Technology, Nanjing 210094, China

(Received 22 August 2022; accepted 30 November 2022; published 12 December 2022; corrected 20 January 2023)

Charm hadrons possess versatile hadro-chemistry as characterized by various transverse-momentum-dependent ratios between their different species. In particular, the charm hadro-chemistry may be modified in relativistic heavy-ion collisions with respect to proton-proton collisions at the same energy, as caused by novel diffusion and hadronization mechanisms of charm quarks in the environment of the created quark-gluon plasma in the former. Inspired by recent measurements of leptons from charm-hadron decays (separated from bottom decays) in Pb-Pb and Au-Au collisions, we investigate the effects of the charm hadro-chemistry on the leptonic observables. We find that full consideration of charm hadro-chemistry in both proton-proton and heavy-ion collisions causes only mild change of charm-leptons' suppression factor with respect to previous calculations hadronizing charm quarks into D mesons only, whereas the resulting change (increase) in the charm-leptons' elliptic flow turns out to be more pronounced as a consequence of the larger collectivity of Λ_c baryons than D mesons.

DOI: 10.1103/PhysRevC.106.064903

I. INTRODUCTION

Heavy-ion collisions at collider energies produce a novel state of deconfined strong-interaction matter that is known as quark-gluon plasma (QGP) and behaves as a strongly coupled near-perfect fluid [1,2]. Heavy quarks, charm and bottom, have masses much larger than the intrinsic nonperturbative scale $\Lambda_{\rm QCD}$ as well as the typical temperatures reached in current heavy-ion collision experiments. Thus they are produced in the initial stage of the collisions and participate in the full evolution of the system (yet with the charm/bottom number conserved), constituting powerful probes of the matter created (for pertinent recent reviews, see [3–6]).

Historically, the traditional observables associated with heavy flavor probes were nonphotonic leptons (electrons and muons) from semileptonic decays of combined charm and bottom hadrons [7–12]. The strong suppression and large elliptic flow of heavy flavor leptons provided evidence of strong coupling of heavy quarks with the medium [13]. In recent years, measurements of charm hadrons have become accessible, which not only corroborated the strong collectivity of charm probes in a more direct fashion [14–21],but also revealed versatile charm hadro-chemistry as characterized by various transverse-momentum (p_T) dependent charm-hadron ratios [22–27]. Interpretation of the strong collectivity and differential hadro-chemistry of charm hadrons requires inputs of charm quark diffusion in the quark-gluon plasma with a rather small spatial diffusion coefficient and hadronization in terms of recombination that plays the dominant role in the low and intermediate p_T regime [28–35].

Going beyond the early measurements of comprehensive heavy flavor leptons, leptons from charm decays have been rather recently separated from those from bottom decays, both in Pb-Pb collisions at $\sqrt{s_{NN}} = 5.02$ TeV by ATLAS collaboration [36,37] and in Au-Au collisions at $\sqrt{s_{NN}} = 200$ GeV by PHENIX [38] and STAR collaborations [39,40], offering an opportunity to test if differential charm hadro-chemistry leaves any imprints on the charm leptonic observables. Indeed in previous studies of heavy flavor leptons [34,41–45], only D mesons were accounted for in the charm quark hadronization and in the ensuing charm decayed leptons. However, from the latest charm hadro-chemistry point of view [29,46], charm quarks are hadronized into different species of charm hadrons that possess varying p_T spectra (including their anisotropy) and have different kinematics and branching ratios when decaying into leptons, leading to possible changes in the charm leptonic observables with respect to the case of hadronizing all charm quarks into D mesons only.

The aim of the present work is to investigate the quantitative effects of full charm hadro-chemistry on the suppression and collective flow of charm leptons. A first attempt in this regard was made in Refs. [47,48], where a schematic charm-baryon-to-meson enhancement in Au-Au collisions (relative to pp collisions) was assumed without taking account of realistic energy loss, and an additional moderate suppression of charm electrons at intermediate p_T was estimated as a result of the smaller branching ratio of Λ_c baryons decaying to electrons than D mesons. In the present work, we employ the full p_T dependent charm hadro-chemistry computed in a comprehensive charm transport approach recently developed in [29] for heavy-ion collisions. For calculating the charm leptons spectrum in pp collisions as the baseline to characterize the medium effect, we use the p_T spectra of various charm hadrons computed in an extended statistical hadronization model [49], which successfully explained the charm hadro-chemistry measured in high-energy pp collisions

*Corresponding author: minhephys@gmail.com

by the ALICE collaboration [50,51]. We find that, with respect to calculations considering charm quarks hadronizing into only D mesons, full consideration of charm hadro-chemistry in both pp and heavy-ion collisions results in only mild change of charm-leptons' nuclear modification factor, while the resulting change (increase) in the charm-leptons' elliptic flow turns out to be more pronounced, which seems to be supported by the recent measurement of charm muons by the ATLAS collaboration [36,37].

The organization of our article is as follows. In Sec. II, we briefly recall the essential ingredients and features of our models developed recently for calculating the charm hadro-chemistry in pp and heavy-ion collisions and show the pertinent results in $\sqrt{s_{NN}} = 5.02$ TeV semicentral Pb-Pb collisions from an updated calculation. In Sec. III, we perform the semileptonic decays of various charm hadrons and compare the corresponding observables between charm muons and their parent hadrons for each species. In Sec. IV, we compare the nuclear modification factor and elliptic flow of total charm leptons computed from all charm-hadron species with the ones calculated from considering charm quarks hadronizing into only D mesons. The quantitative influence of charm hadro-chemistry on charm leptonic observables is then discussed when confronted with pertinent measurements in Pb-Pb and Au-Au collisions. We finally summarize in Sec.V.

II. CHARM HADRO-CHEMISTRY IN *pp* AND HEAVY-ION COLLISIONS

Recent measurements of charm-hadrons differential yields in $\sqrt{s} = 5.02$ TeV pp collisions at midrapidity by the ALICE collaboration demonstrated that charm fragmentation is nonuniversal across different colliding systems, as highlighted by the significant enhancement of the Λ_c^+/D^0 ratio at low p_T relative to e^+e^- collisions [50]. This was successfully explained by an extended statistical hadronization model calculation [49], where the Particle Data Group list of charm baryons was augmented with many more not-yet-observed states predicted from relativist quark model calculations [52]. The p_T spectra of ground state D^0, D^+, D_s^+, and Λ_c^+ were well reproduced and the total charm cross section per unity rapidity (at midrapidity) was fitted to be $d\sigma^{c\bar{c}}/dy \approx 1$ mb, which is consistent with the measured value reported in [51]. These p_T differential cross sections for the ground state charm hadrons will be used to perform semileptonic decays, in order to get the baseline spectra for calculating the nuclear modification factors of the charm leptons in $\sqrt{s} = 5.02$ TeV Pb-Pb collisions.

For the charm hadro-chemistry in heavy-ion collisions, we conduct a calculation within our recently developed transport approach [29]. In this approach, charm quark diffusion in the hydrodynamically expanding QGP was simulated with the transport coefficient calculated in the lattice-constrained T-matrix approach [53,54]. The charm quark hadronization was modelled by resonance recombination; in particular the three-body resonance recombination model (RRM) was developed to compute the charm-baryon formation, taking advantage of the light diquark correlations in the charm-baryon sector. In addition, a method was devised to incorporate space-momentum correlations (SMCs) between the phase space distributions of charm quarks and light quarks that are built up whether through diffusion or from hydrodynamic flow. In practice, the RRM was implemented on an event-by-event basis in combination with the relativistic Langevin simulation of charm quark diffusion in QGP. With the self-consistently determined recombination probability as a function of charm quark momentum in the fluid rest frame, this implementation allows to conserve charm quark number in each event and satisfies both kinetic and chemical equilibrium limits when using thermal quark distributions as inputs. These features, together with the inclusion of all charm-hadron species including augmented charm baryons (same as in pp), are pivotal for controlled predictions of the p_T dependent charm hadro-chemistry.

In Fig. 1, we show the p_T dependence of ground state charm-hadron ratios D^+/D^0, D_s^+/D^0, and Λ_c^+/D^0 in comparison with ALICE data in 30–50% Pb-Pb collisions at $\sqrt{s_{NN}} = 5.02$ TeV, from a calculation within the aforementioned transport model with updated light diquark masses. More specifically, unlike the degenerate diquark masses used in [29], we here use distinct scalar diquark mass ($\approx$710 MeV) for Λ_c states and axial-vector diquark mass ($\approx$909 MeV) for Σ_c states [52]. Such a refinement yields a better description of the p_T shape of the Λ_c^+/D^0 than reported in [29]. Compared to the corresponding ratios in pp collisions [49], D^+/D^0 remains almost the same but D_s^+/D^0 is significantly enhanced in the low and intermediate p_T regime as a result of charm recombination in the presence of strangeness equilibration in QGP [28]. We emphasize here that it is important to correctly reproduce the D^+/D^0 in the present context of studying the hadro-chemistry effects on the charm leptons, since the D^+ semileptonic decay branching ratio is almost two and half times that of D^0 [55]. For Λ_c^+/D^0, the moderate enhancement relative to the pp case only shows up at intermediate p_T due to recombination incorporating SMCs, whereas at low p_T, the value turns out to be compatible with the pp value, implying the integrated ratio may not change [24]. Taken as a whole, we note that these ratios, when integrated over p_T, are consistent with the statistical hadronization model (SHMc) calculations [46] (albeit a smaller Λ_c^+/D^0 value found in SHMc because of less charm-baryons considered therein [46]), as dictated by the *relative* chemical equilibrium reached in the RRM [29].

III. CHARM HADRONS VS DECAYED LEPTONS OBSERVABLES

The calculated ground state charm-hadron p_T spectra are then taken to perform semileptonic decays [43]. More specifically, the semileptonic decays of charm hadrons are simulated as free quark decays $c \to s + l + \bar{\nu}_l$ with the decay matrix element taken from the low-energy $V-A$ theory [56]: $\overline{|\mathcal{M}|^2} \propto (p_s p_{\bar{\nu}_l})(p_c p_l)$ and branching ratios taken from [55]. The quark masses are replaced by the corresponding hadron masses to correctly account for the phase space. The hadronic form factors have little influence on the lepton energy distribution in the parent charm-hadron rest frame [43]. The lepton momenta are then boosted into laboratory frame.

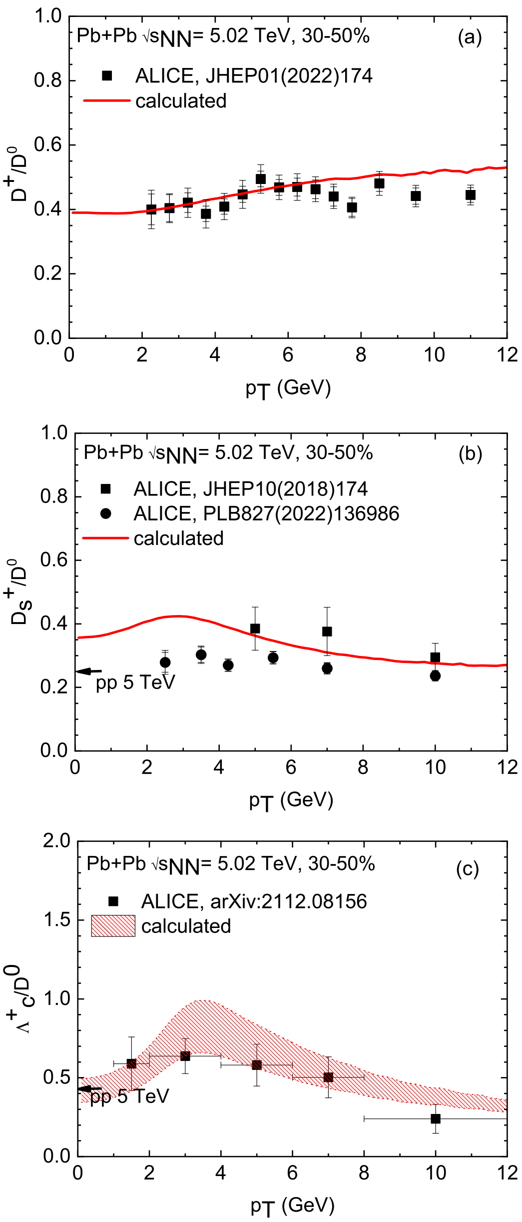

FIG. 1. Calculated charm-hadron ratios in $\sqrt{s} = 5.02$ TeV Pb-Pb collisions in the 30–50% centrality bin at midrapidity in comparison with ALICE measurements [17,23,24]. For Λ_c^+/D^0, the band encompasses uncertainty in the branching ratios of the not-yet-measured excited charm baryons feeding down to the ground state Λ_c^+, taken to be 50–100%, cf. [29].

In Fig. 2, we display the invariant muons spectra decayed from ground state D^0, D^+, D_s^+, and Λ_c^+ spectra that have been normalized to the realistic total charm number $dN_{c\bar{c}}/dy \sim 3.44$ (after taking account of shadowing reduction) in $\sqrt{s} = 5.02$ TeV Pb-Pb collisions in the 30–50% centrality bin at mid-rapidity. One notes that even if the D^+/D^0 is around $\approx$0.4, the invariant muons spectrum decayed from D^+ finally exceeds that from D^0, because the branching ratio of the former ($\approx$16.1%) is almost 2.5 times that of the latter ($\approx$6.5%). The charm muons spectra decayed from D_s^+ and Λ_c^+ are significantly softer than those from D^0 and D^+,

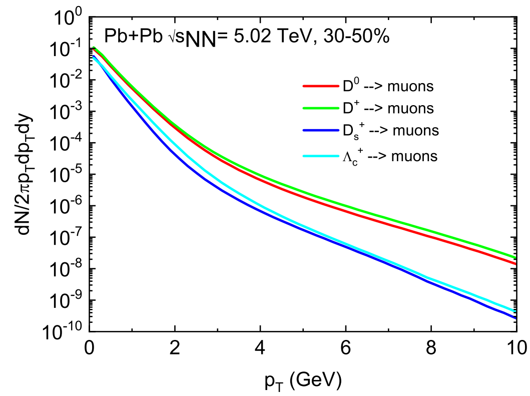

FIG. 2. Charm muons invariant p_T spectra decayed from absolutely normalized p_T spectra of ground state charm hadrons D^0, D^+, D_s^+, and Λ_c^+ in $\sqrt{s} = 5.02$ TeV Pb-Pb collisions in the 30–50% centrality bin at midrapidity. For the case of Λ_c^+, we show only the result corresponding to branching ratios $\approx$100% of excited Λ_c and Σ_c states decaying to the ground state Λ_c^+.

because of the steeper p_T spectra of the former two charm hadrons as well as kinematic effect in the decay associated with their larger masses. This, in combination with the smaller Λ_c^+ semileptonic branching ratio ($\approx$4.5%; the D_s^+ branching ratio is roughly the same as that of D^0), renders the total charm muons spectrum dominated by those decayed from two unstrange charm mesons, which is more so toward high p_T, e.g., at $p_T \approx 1\,(6)$ GeV, the latter accounts for $\approx$70% (90%) of the total. In the present study, we have neglected the contribution from Ξ_c states, since their fraction of total charm cross section is not significant [49].

The nuclear modification factor of a charm hadron is defined as

$$R_{\rm AA}(p_T) = \frac{dN_{\rm AA}/dp_T dy}{N_{\rm coll}/\sigma_{\rm NN}^{\rm in} d\sigma_{\rm pp}/dp_T dy}, \qquad (1)$$

where the numerator is the absolute p_T differential yield of the charm hadron under consideration in heavy-ion collisions, $d\sigma_{\rm pp}/dp_T dy$ is the charm-hadron p_T differential cross section in pp collisions [49] at the same colliding energy, and $N_{\rm coll}$ and $\sigma_{NN}^{\rm in}$ are the binary collision number of the considered centrality bin and the inelastic nucleon-nucleon cross section, respectively. The nuclear modification factors of each charm-hadron species (compared to ALICE measurements) and of their corresponding charm muons are shown in Fig. 3. An overall feature is a shift of the "flow bump" in the well-reproduced charm-hadron $R_{\rm AA}$'s toward lower p_T as a consequence of the decay, which is more significant for the muons from D_s^+ and Λ_c^+ decays.

The elliptic flow coefficient, defined as

$$v_2(p_T) = \left\langle \frac{p_x^2 - p_y^2}{p_x^2 + p_y^2} \right\rangle, \qquad (2)$$

characterizes the momentum anisotropy as a result of charm coupling with the medium through diffusion and hadronization. The v_2 of D^0 (compared to CMS measurements) and Λ_c^+ are shown in Fig. 4 (D^+ and D_s^+ v_2 are similar to that of D^0),

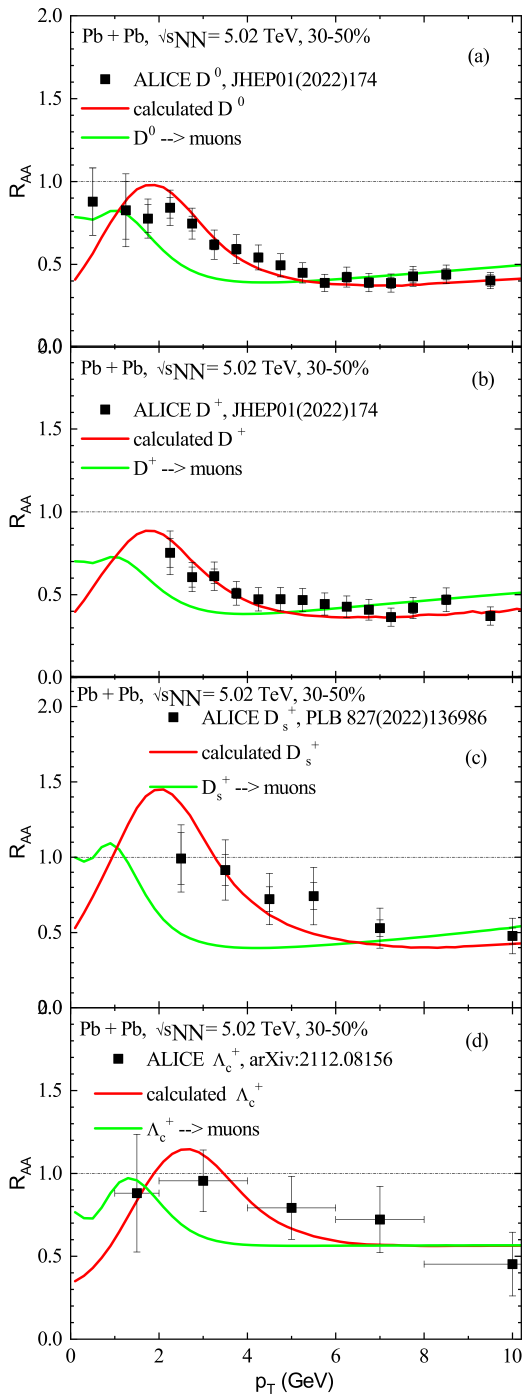

FIG. 3. $R_{\rm AA}$'s of ground state charm hadrons in comparison their corresponding charm muons in $\sqrt{s} = 5.02$ TeV Pb-Pb collisions in the 30–50% centrality bin at midrapidity. ALICE data are taken from [17,23,24]. For Λ_c^+, we show only the result corresponding to branching ratios ≈100% of excited Λ_c and Σ_c states decaying to the ground state Λ_c^+.

together with the v_2 of their decayed muons. An important observation here is that the Λ_c^+ v_2 is significantly larger than that of D^0 toward $p_T > 3$ GeV, as a result of three-body RRM incorporating SMCs that push the reach of recombination to higher p_T [29]. An immediate consequence is that the muons

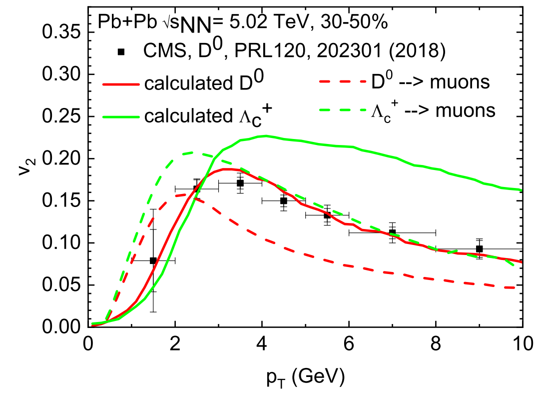

FIG. 4. D^0 and Λ_c^+ v_2 in $\sqrt{s} = 5.02$ TeV Pb-Pb collisions in the 30–50% centrality bin at midrapidity, in comparison with those of their decayed muons. The CMS data of D^0 v_2 are taken from [19].

decayed from Λ_c^+ also have a significantly greater v_2 than the D^0 muons for $p_T > 2$ GeV, which may finally help increase the v_2 of total charm muons.

IV. TOTAL CHARM LEPTONIC OBSERVABLES VS DATA

Having analyzed the observables of charm muons decayed from each charm-hadron species, we are now in a position to combine them together and show the results for the total charm muons. On the other hand, in previous studies of charm leptons within transport approaches [34,41–45], only D mesons (denoting the sum of D^0 and D^+) were accounted for in the charm quark hadronization and therefore in the ensuing charm decayed leptons, ignoring in particular the role of the Λ_c^+ baryons (we have checked that D_s^+/D^0 enhancement as shown in Fig. 1 does not play a significant role in the observables of the final total charm muons, including their v_2, because D_s^+ decayed muons accounts for a rather minor fraction of the total as seen from Fig. 2 and the D_s^+ v_2 is similar to that of the D mesons). Here, for the purpose of making out the pertinent charm hadro-chemistry effects through comparison, we have also conducted a calculation assuming all charm quarks are hadronized into D mesons only, which are then subject to semileptonic decays to get the total charm leptons with an average branching ratio of ≈9.4% (obtained from an average between the branching ratios of D^0 and D^+ using the integrated ratio D^+/D^0 as pertinent weighs). More specifically, we use the charm quark recombination probability into D mesons, $P_D^{\rm coal}(p_c^*)$, self-consistently determined from the RRM formalism [29], and renormalize it to unity at charm quark momentum $p_c^* = 0$ (to ensure low momentum charm quarks are hadronized via recombination [29]), with the remaining $1 - P_D^{\rm coal}(p_c^*)$ identified as the charm quark fragmentation probability into D mesons. This follows the procedure done for the calculation with full charm hadro-chemistry, but in the latter, recombination probabilities of charm quarks into all charm hadrons including the augmented charm-baryon excited states are added up and then renormalized [29].

The calculated $R_{\rm AA}$ and v_2 of the total charm muons are compiled in Fig. 5 in comparison with the ATLAS

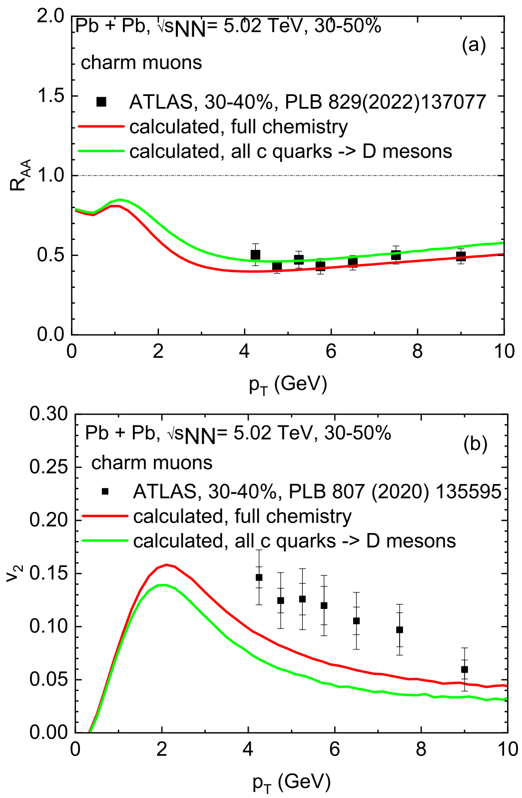

FIG. 5. $R_{\rm AA}$ and v_2 of total charm muons in $\sqrt{s} = 5.02\,\mathrm{TeV}$ Pb-Pb collisions in the 30–50% centrality bin at midrapidity from calculations taking account of full charm hadro-chemistry or from the scenario of charm quarks hadronizing into only D mesons. ATLAS data are taken from [36,37] for charm muons with pseudorapidity cut $|\eta| < 2.0$.

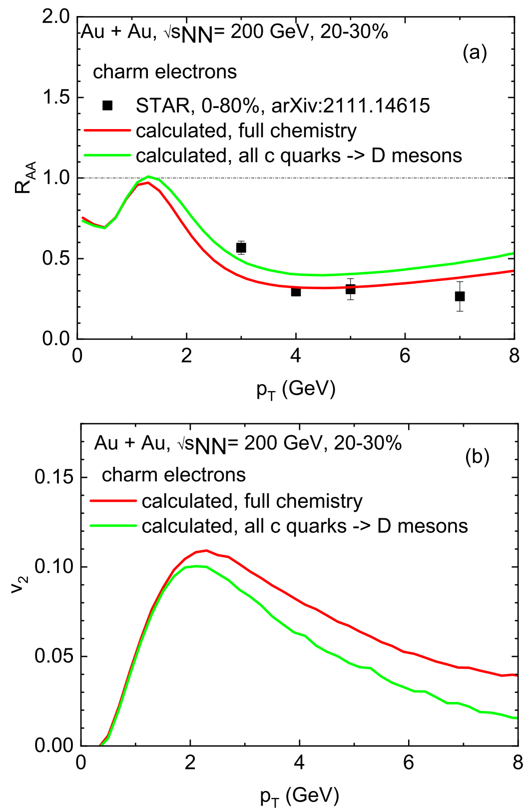

FIG. 6. $R_{\rm AA}$ and v_2 of total charm electrons in $\sqrt{s} = 200\,\mathrm{GeV}$ Au-Au collisions in the 20–30% centrality bin at midrapidity from calculations taking account of full charm hadro-chemistry or from the scenario of charm quarks hadronizing into only D mesons. STAR data are taken from [39].

measurements for $\sqrt{s_{NN}} = 5.02\,\mathrm{TeV}$ Pb-Pb collisions in the 30–50% centrality bin at midrapidity. For consistency, for calculating the R_{AA} in the scenario of all charm quarks hadronizing into D mesons only, we have adopted the same hadro-chemistry in pp collisions as in Pb-Pb collisions, i.e., in pp collisions all charm quarks are fragmented into only D mesons whose p_T spectrum as baseline is normalized to the realistic total charm cross section. One can read from the upper panel of Fig. 5 that taking full account of the charm hadro-chemistry only causes a mild change in the nuclear modification factor of the total charm muons, relative to the scenario of hadronizing charm quarks into D mesons only. The slight increase in the R_{AA} from the latter scenario is mainly caused by the underlying steeper recombination probability function that leads to a slightly harder D-meson spectrum and thus a correspondingly larger D-meson R_{AA}. However, both results are within the error bars of the ATLAS data that are currently limited to $p_T > 4\,\mathrm{GeV}$.

A more pronounced change (increase) in the v_2 of the total charm muons is seen upon full consideration of charm hadro-chemistry, as demonstrated in the lower panel of Fig. 5. This is mostly caused by the significantly greater v_2 of Λ_c^+ and its decayed muons than the D-meson counterparts, cf. Fig. 4. However, this increase is not as large as that seen in Fig. 4, since the total charm muons are dominated by those decayed from D mesons and the contribution from Λ_c^+ accounts only for a minor fraction at intermediate p_T, as demonstrated in Fig. 2. The pronounced increase in the v_2 of the total charm muons as a result of full account of the charm hadro-chemistry seems to be supported by the large value of the ATLAS measurement in the 30–40% centrality, although the present result is still significantly below the ATLAS data in nearly whole measured p_T range.

The same calculations have been performed for $\sqrt{s_{NN}} = 200\,\mathrm{GeV}$ Au-Au collisions in the 20–30% centrality bin as a proxy for the minimum bias collisions [29]. The results for the total charm electrons are shown in Fig. 6. The calculated R_{AA} from full consideration of charm hadro-chemistry is comparable to the STAR data in 0–80% centrality, and the corresponding v_2 is also significantly greater than the result from the scenario of hadronizing charm quarks into D mesons only.

V. SUMMARY

In this work, inspired by the recent measurements of charm leptons by the ATLAS and STAR experiments in Pb-Pb and Au-Au collisions, we have investigated the charm hadro-chemistry effects on the charm leptonic observables within our recently developed transport approach for charm probes [29]. Our study demonstrates that, because the total charm leptons spectrum is still dominated by the ones decayed from D mesons even after taking into account full charm hadro-chemistry, the total charm leptons' nuclear modification factor does not change much as compared to the scenario of hadronizing all charm quarks into D mesons only, which has been widely adopted by transport approaches when computing heavy flavor leptons. Yet the total charm leptons' elliptic flow acquires a pronounced increase because of the inclusion of the Λ_c^+ baryons that have significantly greater collectivity as a result of the three-body recombination, rendering the computed total charm muons v_2 closer to ATLAS data.

Going beyond the charm sector, bottom electrons v_2 has also recently been measured for the first time by the ALICE experiment in Pb-Pb collisions at $\sqrt{s_{NN}} = 5.02$ TeV [57]. Calculated results from transport models [32,33,45] that assumed substantial interactions of bottom quark with the QGP and hadronized bottom quarks into B mesons only significantly underestimated the bottom electron v_2 at intermediate p_T [57], signaling the potentially significant role of Λ_b baryons (through its semileptonic decays) that are expected to have larger collectivity than B mesons. This calls for full and controlled computation of bottom hadro-chemistry in transport approach like for the charm sector [29], which will be addressed in our near-future work.

ACKNOWLEDGMENT

This work was supported by NSFC Grant No. 12075122.

[1] E. Shuryak, Rev. Mod. Phys. **89**, 035001 (2017).
[2] W. Busza, K. Rajagopal, and W. van der Schee, Annu. Rev. Nucl. Part. Sci. **68**, 339 (2018).
[3] X. Dong and V. Greco, Prog. Part. Nucl. Phys. **104**, 97 (2019).
[4] X. Dong, Y. J. Lee, and R. Rapp, Annu. Rev. Nucl. Part. Sci. **69**, 417 (2019).
[5] J. Zhao, K. Zhou, S. Chen, and P. Zhuang, Prog. Part. Nucl. Phys. **114**, 103801 (2020).
[6] M. He, H. van Hees, and R. Rapp, arXiv:2204.09299.
[7] B. I. Abelev *et al.* (STAR Collaboration), Phys. Rev. Lett. **98**, 192301 (2007).
[8] A. Adare *et al.* (PHENIX Collaboration), Phys. Rev. Lett. **98**, 172301 (2007).
[9] S. Sakai (ALICE Collaboration), Nucl. Phys. A **904–905**, 661c (2013).
[10] J. Adam *et al.* (ALICE Collaboration), Phys. Lett. B **753**, 41 (2016).
[11] J. Adam *et al.* (ALICE Collaboration), J. High Energy Phys. **09** (2016) 028.
[12] S. Acharya *et al.* (ALICE Collaboration), Phys. Lett. B **820**, 136558 (2021).
[13] R. Rapp and H. van Hees, Quark-Gluon Plasma **4**, 111 (2010).
[14] J. Adam *et al.* (ALICE Collaboration), J. High Energy Phys. **03** (2016) 081.
[15] B. Abelev *et al.* (ALICE Collaboration), Phys. Rev. Lett. **111**, 102301 (2013).
[16] S. Acharya *et al.* (ALICE Collaboration), Phys. Rev. Lett. **120**, 102301 (2018).
[17] S. Acharya *et al.* (ALICE Collaboration), J. High Energy Phys. **01** (2022)174.
[18] A. M. Sirunyan *et al.* (CMS Collaboration), Phys. Lett. B **782**, 474 (2018).
[19] A. M. Sirunyan *et al.* (CMS Collaboration), Phys. Rev. Lett. **120**, 202301 (2018).
[20] J. Adam *et al.* (STAR Collaboration), Phys. Rev. C **99**, 034908 (2019).
[21] L. Adamczyk *et al.* (STAR Collaboration), Phys. Rev. Lett. **118**, 212301 (2017).
[22] J. Adam *et al.* (ALICE Collaboration), J. High Energy Phys. **03** (2016) 082.
[23] S. Acharya *et al.* (ALICE Collaboration), Phys. Lett. B **827**, 136986 (2022).
[24] S. Acharya *et al.* (ALICE Collaboration), arXiv:2112.08156.
[25] A. M. Sirunyan *et al.* (CMS Collaboration), Phys. Lett. B **803**, 135328 (2020).
[26] J. Adam *et al.* (STAR Collaboration), Phys. Rev. Lett. **127**, 092301 (2021).
[27] J. Adam *et al.* (STAR Collaboration), Phys. Rev. Lett. **124**, 172301 (2020).
[28] M. He, R. J. Fries, and R. Rapp, Phys. Rev. Lett. **110**, 112301 (2013).
[29] M. He and R. Rapp, Phys. Rev. Lett. **124**, 042301 (2020).
[30] S. Plumari, V. Minissale, S. K. Das, G. Coci, and V. Greco, Eur. Phys. J. C **78**, 348 (2018).
[31] S. Cao, K. J. Sun, S. Q. Li, S. Y. F. Liu, W. J. Xing, G. Y. Qin, and C. M. Ko, Phys. Lett. B **807**, 135561 (2020).
[32] M. Nahrgang, J. Aichelin, P. B. Gossiaux, and K. Werner, Phys. Rev. C **89**, 014905 (2014).
[33] W. Ke, Y. Xu, and S. A. Bass, Phys. Rev. C **98**, 064901 (2018).
[34] R. Katz, C. A. G. Prado, J. Noronha-Hostler, J. Noronha, and A. A. P. Suaide, Phys. Rev. C **102**, 024906 (2020).
[35] A. Beraudo, A. De Pace, M. Monteno, M. Nardi, and F. Prino, Eur. Phys. J. C **82**, 607 (2022).
[36] G. Aad *et al.* (ATLAS Collaboration), Phys. Lett. B **807**, 135595 (2020).
[37] G. Aad *et al.* (ATLAS Collaboration), Phys. Lett. B **829**, 137077 (2022).
[38] A. Adare *et al.* (PHENIX Collaboration), Phys. Rev. C **93**, 034904 (2016).
[39] S. Collaboration *et al.* (STAR Collaboration), arXiv:2111.14615.
[40] F. Si, X. L. Chen, L. Zhou, Y. F. Zhang, S. H. Zhang, X. Y. Ju, X. J. Li, X. Dong, and N. Xu, Phys. Lett. B **805**, 135465 (2020).
[41] H. van Hees, V. Greco, and R. Rapp, Phys. Rev. C **73**, 034913 (2006).
[42] P. B. Gossiaux and J. Aichelin, Phys. Rev. C **78**, 014904 (2008).
[43] M. He, R. J. Fries, and R. Rapp, Phys. Rev. C **86**, 014903 (2012).
[44] M. He, R. J. Fries, and R. Rapp, Phys. Lett. B **735**, 445 (2014).
[45] T. Song, H. Berrehrah, J. M. Torres-Rincon, L. Tolos, D. Cabrera, W. Cassing, and E. Bratkovskaya, Phys. Rev. C **96**, 014905 (2017).

[46] A. Andronic, P. Braun-Munzinger, M. K. Köhler, A. Mazeliauskas, K. Redlich, J. Stachel, and V. Vislavicius, J. High Energy Phys. **07** (2021) 035.
[47] P. R. Sorensen and X. Dong, Phys. Rev. C **74**, 024902 (2006).
[48] G. Martinez-Garcia, S. Gadrat, and P. Crochet, Phys. Lett. B **663**, 55 (2008); **666**, 533 (2008).
[49] M. He and R. Rapp, Phys. Lett. B **795**, 117 (2019).
[50] S. Acharya *et al.* (ALICE Collaboration), Phys. Rev. Lett. **127**, 202301 (2021).
[51] S. Acharya *et al.* (ALICE Collaboration), Phys. Rev. D **105**, L011103 (2022).
[52] D. Ebert, R. N. Faustov, and V. O. Galkin, Phys. Rev. D **84**, 014025 (2011).
[53] F. Riek and R. Rapp, Phys. Rev. C **82**, 035201 (2010).
[54] S. Y. F. Liu, M. He, and R. Rapp, Phys. Rev. C **99**, 055201 (2019).
[55] M. Tanabashi *et al.* (Particle Data Group), Phys. Rev. D **98**, 030001 (2018).
[56] D. Griffiths, *Introduction to Elementary Particles* (Wiley & Sons, New York, 1987).
[57] S. Acharya *et al.* (ALICE Collaboration), Phys. Rev. Lett. **126**, 162001 (2021).

Correction: A byline footnote for the second author was missing and has been inserted.